An analysis ~~on~~ of temporal scaling ~~behavior~~ behaviour of extreme rainfall ~~of~~ in Germany based on radar precipitation QPE data

Judith Marie Pöschmann[1], Dongkyun Kim[2], Rico Kronenberg[1], and Christian Bernhofer[1]

[1]Department of Hydrosciences, Institute of Hydrology and Meteorology, Technische Universität Dresden, 01069 Dresden, Germany

[2]Department of Civil and Environmental Engineering, Hongik University, Wausanro 94, Mapo-gu, Seoul, 04066, Korea

Correspondence: Judith Pöschmann (Judith.Poeschmann@tu-dresden.de)

Abstract. We investigate the depth–duration relationship of maximum rainfall over the whole of Germany based on 16 yrs of radar derived Quantitative Precipitation Estimates (namely, RADKLIM–YW, German Meteorological Service) with a space–time resolution of 1~~km~~ km^2 and 5 min. Contrary to the long–term historic records that identified a smooth power law scaling ~~behavior~~ behaviour between the maximum rainfall depth and duration, our analysis revealed three distinct scaling regimes of which boundaries are approximately 1 h and 1 d. Few extraordinary events dominate a wide range of durations and deviate to the usual power law. Furthermore, the shape of the depth–duration relationship varies with the sample size of randomly selected radar pixels. A smooth scaling ~~behavior were~~ behaviour was identified when the sample size is small (e.g. 10 to 100), but the original three distinct scaling regimes became more apparent as the sample size increases (e.g. 1 000 to 10 000). Lastly, a pixel wise classification of the depth–duration relationship of the maximum rainfall at all individual pixels in Germany revealed three distinguishable types of scaling ~~behavior~~behaviour, clearly determined by the temporal structure of the extreme rainfall events at a pixel. Thus, the relationship might change with longer time series and can be improved once available.

1 Introduction

Extreme rainfall poses significant threats to natural and anthropogenic systems (Papalexiou et al., 2016). The frequency and magnitude of extreme rainfall are expected to increase in the future (Blanchet et al., 2016; Gado et al., 2017; García-Marín et al., 2012; Ghanmi et al., 2016; Lee et al., 2016; Madsen et al., 2009; Marra and Morin, 2015; Marra et al., 2017; Overeem et al., 2009; Yang et al., 2016) especially at sub–daily timescales ~~(Fadhel et al., 2017; Westra et al., 2013, 2014) to which fatal and frequent disasters such as urban~~(Barbero et al., 2017; Fadhel et al., 2017; Guerreiro et al., 2018; Westra et al., 2013, 2014) leading potentially to more urban and non-urban flash floods (Dao et al., 2020), riverine floods, and landslides ~~sensitively react. Therefore, a~~ A thorough understanding on magnitude, duration, and frequency of extreme rainfall is ~~imperative~~ thus necessary for efficient design, planning, and management of these systems~~.~~, with many needing (sub–)hourly information especially.

Obstacles to identifying and investigating extremes and record rainfall events are their rare occurrence as well as the spatiotemporal resolution and coverage of rainfall information in general. Lengfeld et al. (2020) analysed the problems of rain gauge observations, missing more than 50 % of the extreme rainfall events observed, with even more missed at higher

temporal resolutions. Remotely sensed precipitation products with high spatiotemporal resolution such as the ones provided by radar, satellite or microwave link networks may solve this issue. For rainfall extremes, weather radar systems are seen to be appropriate to capture the spatial variability and extreme events with limited spatial extent (Borga et al., 2008). However, most of the currently available radar QPE (quantitative precipitation estimates) data sets do not cover very long periods (Lengfeld et al., 2020), while their high spatiotemporal resolution is superior to many other rainfall products. Radar products also have well–known uncertainties, like variation of reflectivity with height, relating radar reflectivity to precipitation rates, clutter and beam blocking. Therefore, their processing is subject to improvements, and reprocessing these data sets is necessary in order to achieve homogeneous and consistent products that can be evaluated for rainfall characteristics over space and time.

Probable maximum precipitation (PMP) is one way to define extreme rainfall. It is defined as the theoretically greatest depth of precipitation for a given duration that is physically possible over a particular drainage basin at a particular time of year (Ralph E. Huschke, 1959). ~~The PMP is primarily used while designing important hydraulic structures such as major dams where breaking or failure would result in significant loss of lives and properties downstream. The PMP is estimated in three different ways. First, the hydro–meteorological method can be applied. In this method, the maximum precipitation event that was observed at or nearby the location of interest is adjusted to account for the simultaneous occurrences of the most critical meteorological conditions (e.g. dew point, temperature, wind, and air pressures, etc.). Second, the statistical method fits the series of the annual maximum rainfall values to a given probability density function, and then the rainfall with extremely high recurrence interval (e.g. 10 000 yr) is estimated from the probability density function, which is considered as the PMP. Last, the~~ One of the methods to estimate the PMP is the maximum rainfall envelope curve method, that plots the depth (y)–duration (x) relationship of the record rainfall events observed across a large geographical boundary (e.g. entire country or globe) on the log–log plane. ~~Then,~~ The PMP is then derived as a straight line on the plot representing the upper boundary of the envelope containing all depth–duration relationships~~is estimated as the PMP. The~~ . This maximum rainfall envelope curve method was first proposed by Jennings (1950), ~~which~~ who showed that the depth of the extreme rainfall events observed across the globe is a power function of their duration. ~~This relationship~~ Jennings discovered that this unique scaling behaviour holds at rainfall durations between 1 min through 24 months. Paulhus (1965) showed that the same power law relationship holds after the addition of a new world rainfall record observed at the island of La Réunion at the duration between 9 h and 8 d. The envelope for these extreme values can be expressed as~~follows~~:

$$pP = \alpha dD^{\beta} \tag{1}$$

where ~~p~~ P is the maximum precipitation (in mm) occurring in duration ~~d~~D (in h), the coefficient α ~~represents the y intercept~~ (425 in Paulhus (1965)) represents the value at one hour of the depth–duration relationship plotted on the log–log plane, and the exponent β (0.47 in Paulhus (1965)) is the parameter characterizing the scaling ~~behavior~~ behaviour of the depth–duration relationship. ~~Parameters α and β have the value of 425 and 0.47 (for D in hours), respectively, for the analysis performed on the multiple extreme rainfall events observed across the globe. Jennings discovered that this unique scaling behavior holds at the rainfall duration between 1 min through 24 months. Paulhus (1965) showed that the same power law relationship holds after~~

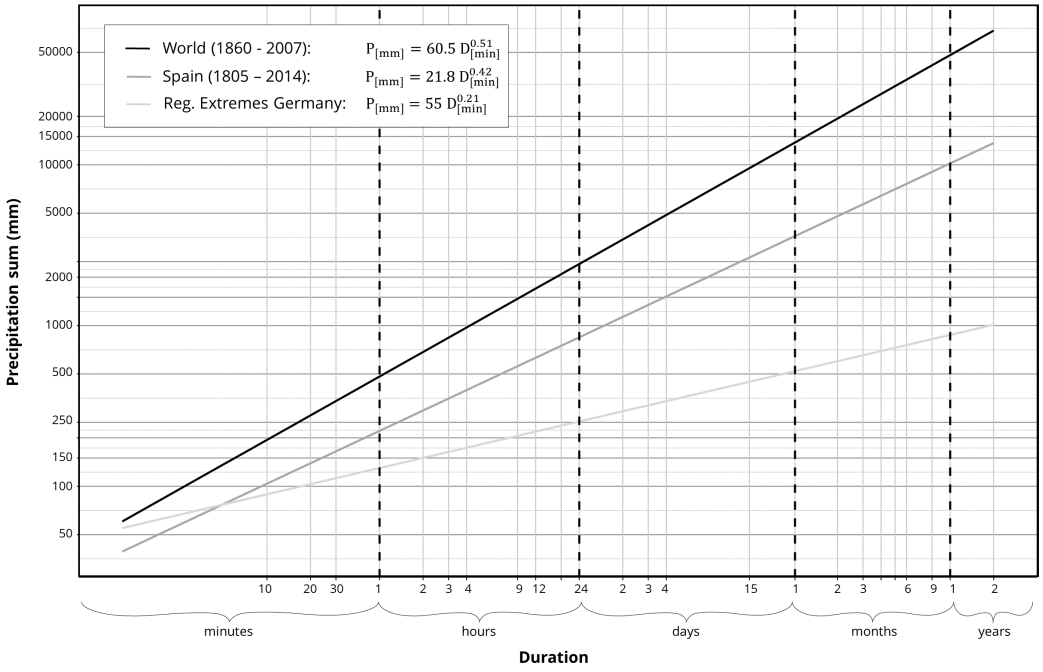

Figure 1. ~~Extreme~~ Scaling relationships of extreme (record) precipitation values for different durations ~~: World extremes (World Meteorological Organization, 1994)~~based on worldwide data (World Meteorological Organization, 1994; NWS, 2017; Gonzalez and Bech, 2017), Spanish ~~extremes~~ rain gauge data (Gonzalez and Bech, 2017), and a regional ~~extremes for~~ analysis of Eastern Germany (Dyck and Peschke, 1995)

~~addition of new world rainfall record observed at the island of La Réunion at the duration between 9 h and 8 d~~The Spanish study of Gonzalez and Bech (2017) updated the world envelope's slope to 0.51, showing a remarkable stability. Multiple exponents describing the scaling property of extremes have been retrieved at various regions around the world (Commonwealth of Australia, 2019; Gonzalez and Bech, 2017). Figure 1 shows the maximum rainfall–duration relationship identified by some of these studies. All relationships reveal power law relationships, with exponents around ~~0.45~~ 0.5 (Spanish and global estimate) and 0.2 (German) over a wide range of scales.

Several studies examined the validity of this universal scaling exponent. Galmarini et al. (2004) showed, based on the rainfall records observed at several stations in Canada, Australia, and La Réunion, that the single exponent scaling laws exist only for single stations experiencing extremely high precipitation and that the deviation from a scaling law is caused by the intermittency associated with a substantial number of zero precipitation intervals in data. They also showed that the scaling exponent β tend to stay around 0.5 based on the stochastic simulation assuming a point rainfall process composed of the Weibull distributed rainfall depth and a given temporal autocorrelation structure. Zhang et al. (2013) showed that the scaling exponent varies around 0.5, if the vertical moisture flux and rainfall can be ~~modeled as the AR(1) and the truncated~~modelled by

a censored (or truncated) first–order autoregressive process AR(1)~~stochastic process~~. However, these works showed the scaling ~~behavior~~ behaviour of maximum rainfall at a single point location, and did not investigate maxima observed at different spatial locations.

One of the main obstacles to identify the "true" scaling ~~behavior~~ behaviour of maximum rainfall is that the most rainfall is measured from sparse ground gauge networks (Dyck and Peschke, 1995; Papalexiou et al., 2016). ~~Remotely sensed precipitation products with high spatio–temporal resolution such as the ones provided by radar, satellite or microwave link networks may be applied to overcome this issue.~~ Breña-Naranjo et al. (2015) used a satellite based rainfall product to identify the scaling ~~behavior~~ behaviour of the maximum rainfall across the globe. They showed that the maximum of the areal rainfall averaged over the ~20 km × ~20 km data grid has the scaling exponent of ~0.43 which is similar to that of Jennings (1950)~~while the maximum rainfall values were systematically underestimated. They attributed the main reason of the discrepancy to the~~ . However, the coarse spatial resolution of the satellite data ~~that~~ easily misses the small scale rainfall variability that is closely associated with extreme values, thus the found extremes in the satellite data are lower than expected (Cristiano et al., 2017; Fabry, 1996; Gires et al., 2014; Kim et al., 2019; Peleg et al., 2013, 2018).

~~Taken these findings, we want to analyze~~ In this study, we analyse the rainfall depth–duration relationship for the whole of Germany based on ~~the~~ 16 ~~y of the Quantitative Precipitation Estimates (QPE)~~ years of RADKLIM–YW, a carefully reprocessed QPE radar product with 1 km–5 min space–time resolution~~in order~~ . We want to answer the following questions regarding the scaling ~~behavior~~ behaviour of the maximum rainfall: (1) Does the depth–duration relationship of German extreme rainfall show scale invariant ~~behavior~~behaviour? If so or if not, what is the primary reason? (2) Does this relationship vary with regard to the spatial sampling rate? (3) Does it provide any clue to modify the relationship currently applied in practice based on sparse gauge ~~network~~networks? The answers to these questions would be especially intriguing because few studies have so far investigated the scaling ~~behavior~~ behaviour of maximum rainfall based on such a high spatio–temporal resolution rainfall ~~data~~ dataset recorded over a long period and a large spatial extent as this study did. ~~In addition, the practicality of the result would add value to this study. This is especially because the depth–duration relationship of the extreme rainfall of Germany revealed by our extensive QPE radar data analysis may be used to modify the current design guidelines regarding the PMP.~~

2 Data and Methods

2.1 Data Description

2.1.1 ~~Quantitative Precipitation Estimates (QPE)~~

The German National Meteorological Service (DWD) ~~has been~~ is running a radar network (currently ~~18~~ 17 C–band radars) for almost two decades and is providing different ~~free and purchasable~~ rainfall data derived from it. Full coverage of Germany has not been reached until today, however, all ~~neighboring~~ neighbouring countries contribute to the rainfall information and the extension of the network is ongoing. One QPE from German radar data is a Radar Online Calibration called RADOLAN (German: RADar OnLine ANeichung), which combines ground ~~near~~ information of fallen precipitation (rain

gauge data) with radar data. ~~The RADOLAN product is going through quality enhancements since 2005. A~~ Since the quality enhancement of RADOLAN is ongoing without post–correcting previous data, the so–called radar climatology project of the DWD, RADolanKLIMatologie (RADKLIM, Winterrath et al., 2017) has consistently ~~reanalyzed~~ reanalysed the complete radar ~~data~~ archive set since 2001 ~~to attain homogeneity of the data that were processed through different algorithms.~~ for improved homogeneity despite the originally different processing algorithms. Compared to RADOLAN, RADKLIM has implemented additional algorithms leading to consistently fewer radar artefacts, improved representation of orography as well as efficient correction of range–dependent path–integrated attenuation at longer time scales (Kreklow et al., 2019). Whereas RADOLAN is not well suited for climatological applications with aggregated precipitation statistics, RADKLIM is a promising data set for these climatological applications. The RADKLIM data is available in the following two formats with around 392 128 filled pixels within the German border: 1) RADKLIM–RW is an hourly precipitation product resulting from radar based precipitation estimates that are calibrated with ground stations (Winterrath et al., 2018a), which was validated by several studies, such as Lengfeld et al. (2019) and 2) RADKLIM–YW (Winterrath et al., 2018b) is a 5 min product resulting from a correction/factoring of DWD's 5 min product RADOLAN–RY (rainfall estimate after basic quality correction and refined z–R–relationship) with the help of ~~RADOLAN–RH and~~ RADKLIM–RW on a sequential hourly base. The RADKLIM–YW version 2017.002 was used in this study due to its high temporal resolution necessary for the analysis. It is already the third version, covering the years 2001 to 2018. Due to comparison reasons with another study at our institute, only years 2001 to 2016 had been used for this study. The YW product covers the area composed of 1100~~x~~ x 900 pixels with the spatial resolution of 1 km (improved compared to former version of RADOLAN). ~~For more information on the RADKLIM~~ Remaining weaknesses of RADKLIM (as outlined in Kreklow et al. (2019)) are the greater number of missing values (compared below) compared to RADOLAN as well as negative bias causing an underestimation of high intensity rainfall due to spatial averaging and rainfall–~~YW, see Kreklow et al. (2019).~~ induced attenuation of the radar beam.

2.1.1 ~~Data processing and quality issues~~

The data comprises 75.2 GB of compressed raw binary data (one layer for each time step) for 2001 to 2016, making 3.43 TB of unpacked data. Since not all raster ~~cells~~ pixels are with values (only around half of the values lay within the borders of Germany), the spatial data was converted to time series for quicker processing. ~~Analysis was conducted in R (R Core Team, 2019) and Matlab, with figures produced using ggplot (Wickham, 2016) and RasterVis (Perpiñán and Hijmans, 2019). The fst format (Klik, 2019) was chosen to store the data . The data contains the~~ The data contains missing values (~~NA~~NaN) of the following two types: 1) ~~NAs~~ NaNs due to changes and ongoing extension of the radar network. This mainly affects areas near the border of Eastern, Northern, and Southern Germany. Some time series are, for example, only available from 2014 onwards. 2) Some locations/raster ~~cells have NA values~~ pixels have NaNs potentially due to malfunction of the radar or general (radar) errors. Figure 2 (a) shows the proportion of the ~~NA values~~ NaNs of the time series developed for each of the pixels. The visible cones display the individual radar coverage, and the overlapping areas of the radar cones have a better data coverage than the areas without overlapping. Additionally, Fig. 2 (b) shows the maximum rainfall differences between right before and after a data gap,

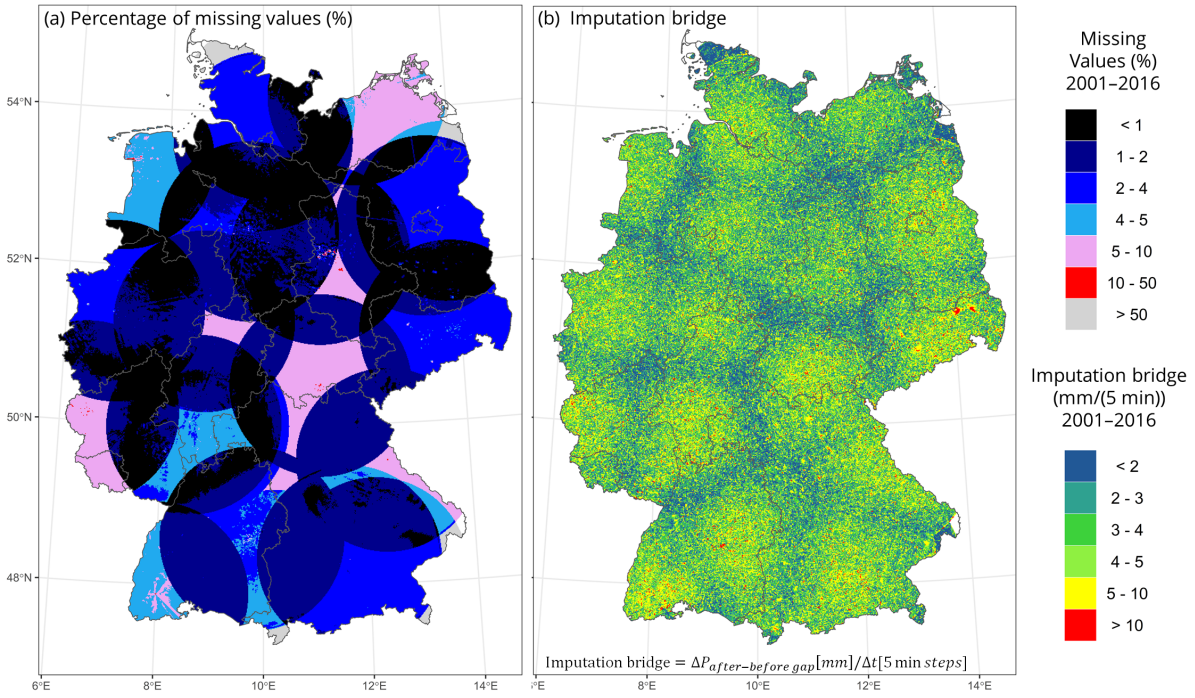

Figure 2. ~~Spatial distribution~~ Results of ~~the proportion~~ NaN analyses of ~~missing values for~~ the QPE RADKLIM–YW from 2001~~–~~2016: (a) ~~Percentage~~ Spatial distribution of ~~missing values~~ the proportion of NaNs (in %) for each pixel, (b) Maximum intensity per time step of 5 min that need to be interpolated (= maximum intensity difference within one time step to overcome). The German boundary is obtained from the GADM Global Administrative Database (Hijmans et al., 2018) .

calculated for a time step of 5 min (Imputation bridge = Intensity difference/gap length). The red spots could mean a difference of greater than 180 mm h^{-1}.

~~There are multiple options of handling missing values, but it is very~~ It is hard to handle NaNs in highly episodic geophysical events such as rainfall. ~~Even harder is the imputation of NA values which might be potential extreme rainfall events. We chose not to do any correction~~Based on Fig. 2, we chose to not do any data interpolation, since the ~~distribution of the imputation bridge is sporadic, which means that the maximum values that could have been missed at one pixel would be complemented by the observation at the adjacent pixel. Furthermore, the worst consequence of this approach would mean the missing of an extreme value whereas the consequences of~~ consequence of imputing potentially too high extreme values ~~seemed~~ is more severe and uncertain for our study than the missing of any extreme values.

2.2 ~~Methodology~~Depth–Duration relationships

2.2.1 ~~Estimation of maximum rainfall at each radar cell~~

Maximum rainfall ~~intensities were retrieved from aggregating the 5 min~~ values for each duration ~~τ of interest with moving window sampling~~ τ between 2001–2016 were calculated with rolling sums applied over moving windows using the R~~package RcppRoll~~ –package Rcpp–Roll (Ushey, 2018). Durations of up to 3~~h~~ d were chosen for the analysis, with multiple steps for ~~min and h~~ minutes and hours out of our interest for sub–hourly and sub–daily pattern. The ~~values~~ records may include non–rainfall data and thus do not imply continuous precipitation for the period considered. Values were not aggregated spatially, since this usually reduces the maximum intensity values (Cristiano et al., 2018).

~~The radar data can be expressed as~~

~~$X = \{\{X_1,...,X_{n_P}\}_1,\{X_1,...,X_{n_P}\}_2,...\{X_1,...,X_{n_P}\}_N\}$ with N being the number of pixels for whole Germany and n_p the number of observation in time series.~~

~~For one single time series/raster cell the values $\{X_1,...,X_{n_p}\}_{cell}$ are aggregated for each τ according to Eq. (??), p being the index for each aggregated sample:~~

~~$M_{\tau,p,cell} = \sum X_{i=p}^{p+\tau-1}\{X_i\}_{cell}, p = 1,2,..(n_P - \tau + 1)$~~

~~The maxima for each τ are retrieved with Eq. (??).~~

~~$M^{(\tau)}_{\max,cell} = \max\left\{M^{(\tau)}_1,..,M^{(\tau)}_{(n_P-\tau+1)]}\right\}_{cell}$~~

2.2.1 ~~Depth–Duration relationship for whole Germany~~

~~Finally~~First, the extreme values for each pixel and duration $M^{\tau,pixel}_{\max}$ are calculated. Afterwards, the overall maxima for whole Germany for each τ ~~are taken from each time series' maxima according to Eq. (??)~~ ($M^{(\tau)}_{\max}$) is extracted from these calculated extreme values. Based on these results, the depth–duration relationships can be built for each pixel as well as for the whole of Germany.

~~$M^{(\tau)}_{\max} = \max\left\{M^{(\tau)}_{\max,1},..,M^{(\tau)}_{\max,N}\right\}$~~

~~The scaling relationship with scaling factor b and intercept B can be established as following.~~

~~$\log(M^{(\tau)}_{\max} = B + b \cdot \tau$~~

~~respectively~~

~~$M^{(\tau)}_{\max} = 10^B \cdot b$~~

2.3 K–Mean Clustering of Depth–Duration–Relationships

2.3.1 ~~K–Mean Clustering of Depth-Duration-Relationships~~

The depth–duration relationships ($M^{\tau,pixel}_{\max}$ vs τ) for each pixel derived from Sect. ~~??~~ 2.2.1 are individually clustered with the K–Mean clustering algorithm (Scott and Knott, 1974). ~~Erroneous pixels (due to too many NA values in the time series~~"Erroneous" pixels (=having NaNs as resulting maxima) were excluded from the cluster process in order to avoid ~~disturbance~~disturbances.

The data was rescaled to make the characteristics more comparable with each other. ~~The elbow evaluation (compare Fig. ?? for estimating the best~~ If the number of clusters ~~gave no obvious suggestion (~~is not predefined, it can be identified by drawing an elbow chart.For different numbers of clusters K the measure of the variability of the observations within each cluster (Total within–cluster sum of squares, y–axis) is calculated and the curve should bend like an elbow ~~). We~~ at the optimal value. Since the algorithm did not suggest a number of clusters, we chose six clusters for a sufficiently detailed analysis since it gave consistent results when repeating the automatic algorithm for several times (each time the algorithm clusters slightly differently).

~~Elbow evaluation for K–Mean Clustering carried out for the rescaled maximum rainfall values~~

3 Results and discussion

3.1 Scaling ~~behavior~~ behaviour of entire Germany

Figure 3 shows the maximum depth–duration relationship of the entire Germany that was derived from the QPE radar data (~~blue solid line~~dots). The same relationship based on ground gauge network (~~red dotted line~~empty triangles) and the world ~~record~~ records (filled triangles) are shown for reference. The rain gauge based values clearly follow a scaling relationship with a slope that is different in comparison to world extremes. Radar based maxima for the shorter duration from 2001 to 2016 do not cover all sub–daily extremes but exceed observed ones from the 1 d durations as well as for ~~some~~ one sub–daily ~~values~~value. In Fig. 3, a "plateau" is visible between around 35 min up to 18 h, indicating a "one event" effect at 35 min, potentially from an extreme rainfall event in this period. Overall, a scaling ~~behavior~~ behaviour can be observed at sub–hourly durations with a scaling component of around 0.65 even though the maxima ~~were observed at very distant places~~ are observed rather randomly across the whole of Germany as indicated by the map showing the location of the maximum rainfall. This result implies that even though the location of extreme rainfall is different, the maximum rainfall may exhibit smooth scaling ~~behavior~~ behaviour if the rainfall generation mechanism is similar. As mentioned in the data quality description, it is possible that these sub–hourly values do not represent the true extremes across Germany for 2001–2016 since radar–based measurements at fine timescale (e.g., xx minutes) are highly sensitive to the averaging effects. Between 25 min and 16 h, maximum values are calculated for ~~the southeastern edge~~ a location at the border of Hesse state ~~in May 29th 2016. These very high values at this specific location are not~~ and Bavaria in August 25th 2006, which has not been documented in public news~~, however there had been severe weather around that time~~. The extreme event around ~~June 29th, 2017 at~~ September 30th, 2003 around Berlin comprised the maximum depth–duration relationship at the duration between 18 h and 2 d. The weak scaling ~~behavior~~ behaviour existed in the regime at the 18 h and 3 d duration with the scaling exponent of 0.20.

3.2 ~~Scaling behavior of entire Germany for high–quantile rainfall~~

All maximum locations and the corresponding dates of occurrence are provided in Table 1.

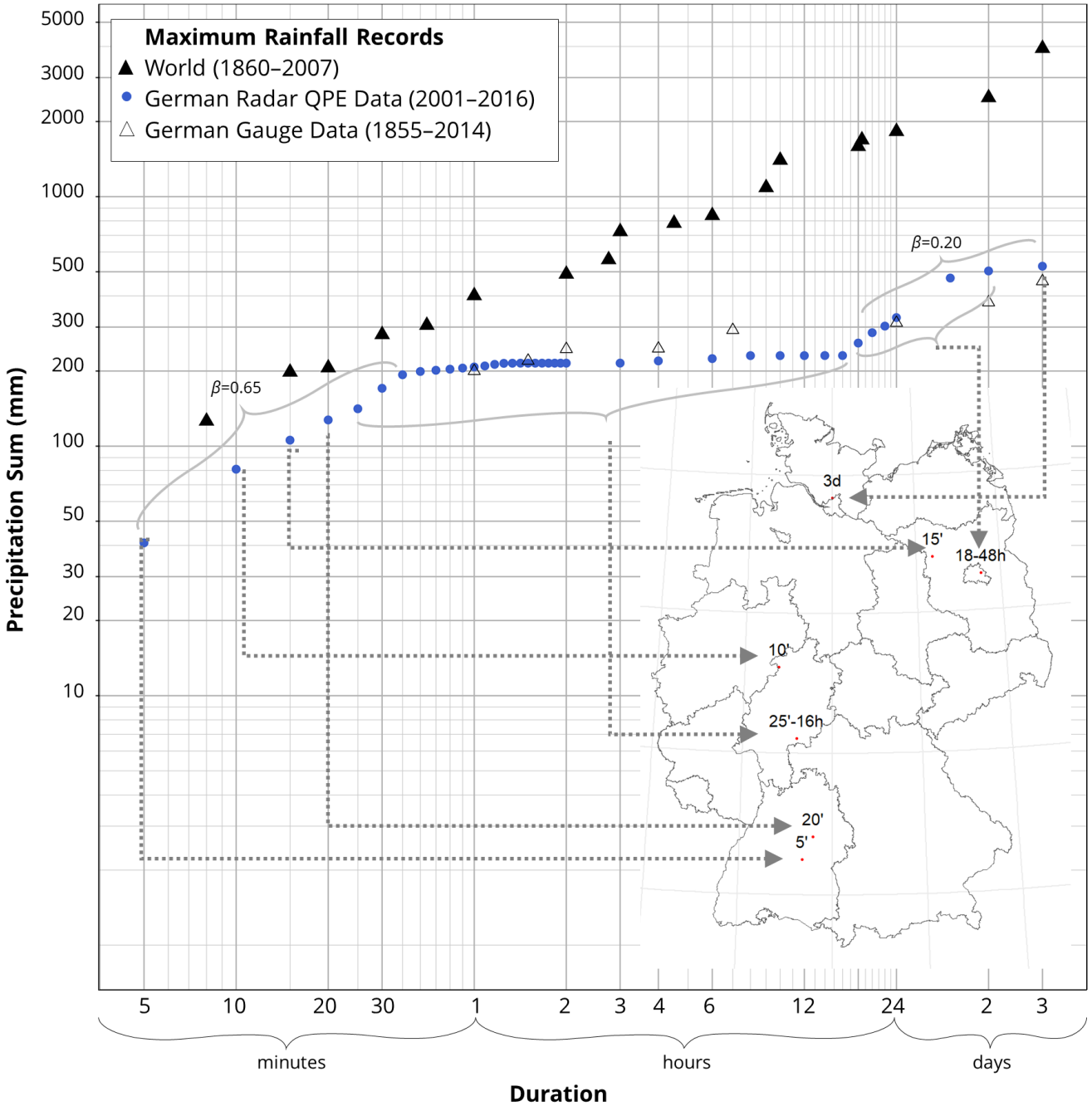

Figure 3. Overview of maximum rainfall records in Germany. Chart: Maximum depth–duration ~~relationships and locations~~ relationship of rainfall ~~maxima. Lines: German radar derived~~ records based on QPE RADKLIM–YW (data of this study) (blue dots), and as reference the relationships based on the German ground network ~~(DWA, 2015; DWD, 2002, 2016), Spanish ground gauge records (Gonzalez and Bech, 2017),~~(Rudolf and Rapp, 2003; DWA, 2015; DWD, 2020) (non–filled triangles) and the "world records~~(World Meteorological Organization, 1994)~~" (World Meteorological Organization, 1994; NWS, 2017). Map: Locations of rainfall maxima (based on ~~the German radar data~~QPE RADKLIM–YW) for the considered duration.

Table 1. Rainfall records for different duration from RADKLIM–YW for 2001–2016 with corresponding locations.

Duration	Start Date	Start Time (Time Zone: Berlin)	Precipitation Sum (mm)	Location (WG84)
5 min	2009–07–04	2:10 PM	40.94	48.50015° N, 9.35161° E
10 min	2006–07–07	9:30 AM	80.82	51.22436° N, 8.767699° E
15 min	2010–07–12	11:05 PM	105.61	52.79713° N, 12.39296° E
20 min	2002–07–30	5:15 PM	127.32	48.82225° N, 9.577044° E
25 min–16 h	2006–08–25	05:25 AM–1:25 PM	141.13–230.67	50.21148° N, 9.201292° E
18 h–1 d	2003–09–29	09:05 AM–03:05 PM	258.91–327.45	52.52761° N, 13.5271° E
1.5–2 d	2003–09–28	02:20–9:35 PM	471.67–503.66	52.52761° N, 13.5271° E
3 d	2001–04–08	06:50 AM	525.89	53.67822° N, 10.00056° E

Maxima of 25 min–16 h as well as from 18 h–2 d correspond to the same location and date and are thus summarized.

3.2 Scaling behaviour of entire Germany for high–quantile rainfall

High rainfall values are associated with especially great uncertainty when obtained from radar data. Thus, we also investigated the scaling ~~behavior~~ behaviour of high–quantile rainfall values. Figure 4 shows the maximum depth–duration relationship of several quantiles: 0.99999 (fourth greatest ~~cells~~pixel value), 0.9999 (39th greatest ~~cells~~pixel value), 0.999 (392nd greatest ~~cells~~pixel value), and 0.99 (3921st ~~cells~~greatest pixel value). The "three phase regime" from radar maximum values remains relatively stable, however, the "single event" effect between 50 min and 1 d is smoothed out, because the degree of inflections in the curve becomes weaker. ~~The lower the chosen quantile, the clearer the scaling regime appears~~Lower quantiles thus show a smoother curve rather than the 3–regime form.

Figure 5 shows the location of the ~~0.9999~~0.99999, 0.9999, 0.999, and 0.99 quantile rainfall. The ~~color~~ colour of the circles represents the different rainfall durations. ~~The lower the quantile, the sparser the location of the quantile rainfall occurrence, which~~ It shows that the number of locations increases the lower the maximum rainfall quantile is. This suggests the reduction of the influence of one single rainfall event on the depth–duration relationship causing inflection in the curve.

~~The map corresponding to the lower quantiles (e.g.~~ Additionally, from a certain degree of quantile (Fig. 5 (~~c) and 5 (~~d)) ~~reveals that~~ the locations of maximum rainfall contributing to the development of the rainfall–duration relationship ~~are spread over the whole of Germany.~~ seem to happen mainly in the wider Alpine region in South Germany. This suggests that natural rainfall mechanisms are dominating the scaling relationship, such as regional characteristics and meteorological conditions (e.g. orographic lifting or leewards effects). Naturally, one would assume that this heterogeneity of the meteorological conditions and rainfall generating mechanisms will reflect ~~rather~~ regional characteristics and will exhibit some irregular scaling ~~behavior~~behaviour. Contrary to this conjecture, the ~~curve shows a very smooth scaling behavior, that suggests the extreme rainfall events at this degree of quantile (upper one percentile) share common characteristics such as peak rainfall depth and correlation structures regardless of timescale that could have been derived from similar generation mechanisms~~curves in Fig. 4 (99.9 % and 99 %) show a quite smooth scaling behaviour.

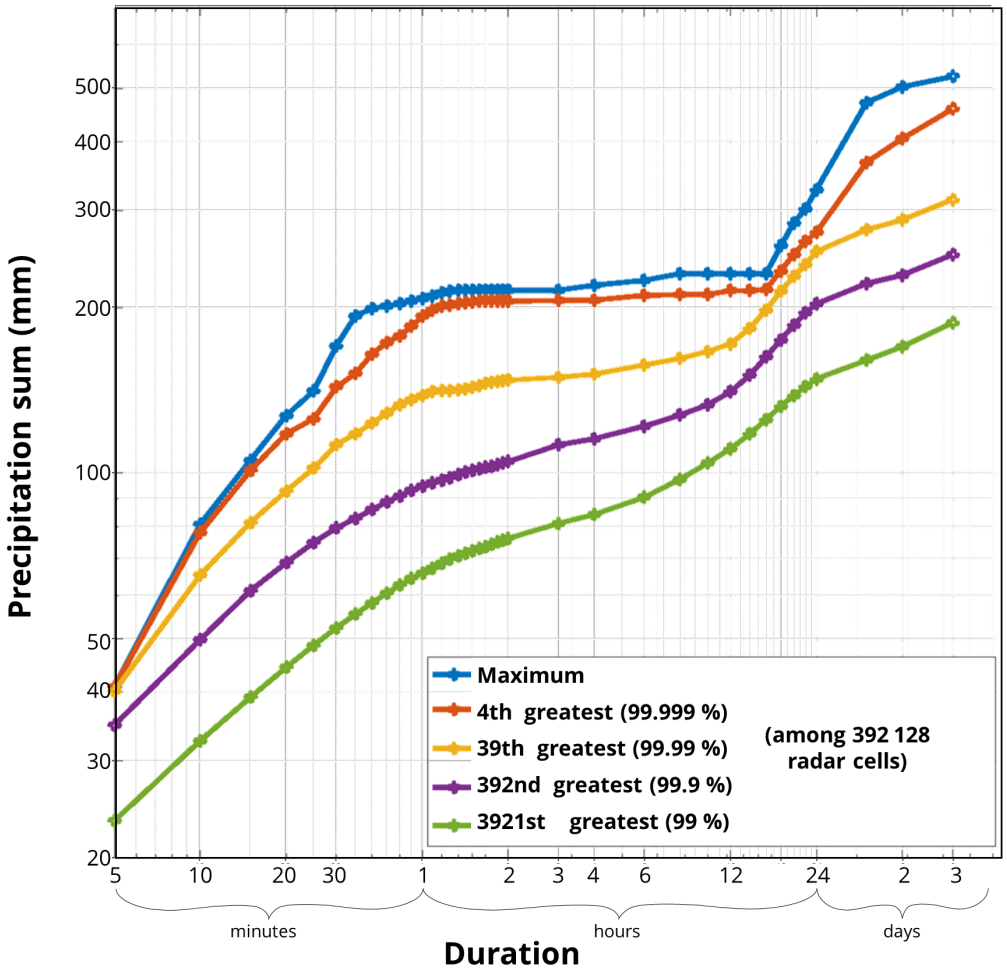

Figure 4. Depth–duration ~~relationship~~ relationships of ~~the maximum~~ rainfall values of whole Germany based on QPE RADKLIM–YW for 2001–2016 from maximum values down to the 3921st greatest per duration.

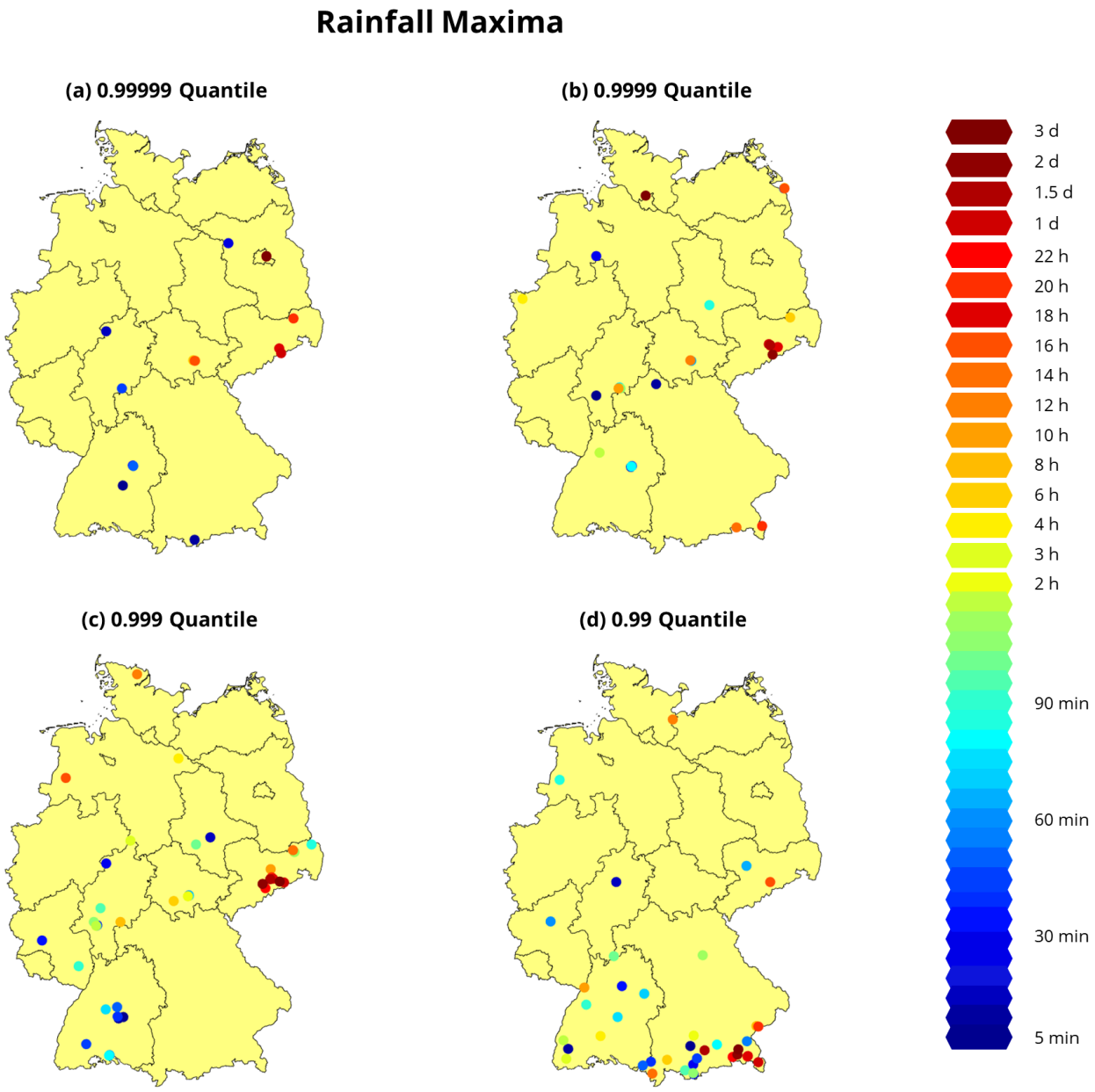

Figure 5. Locations of the 0.99999, 0.9999, 0.999, and 0.99 quantile rainfall with varying durations from 5 min to 3 d. Point ~~colors~~ colours represent the corresponding rainfall duration, similar for each quantile. Different numbers of data points in panels a–d result from several data points being at the same location.

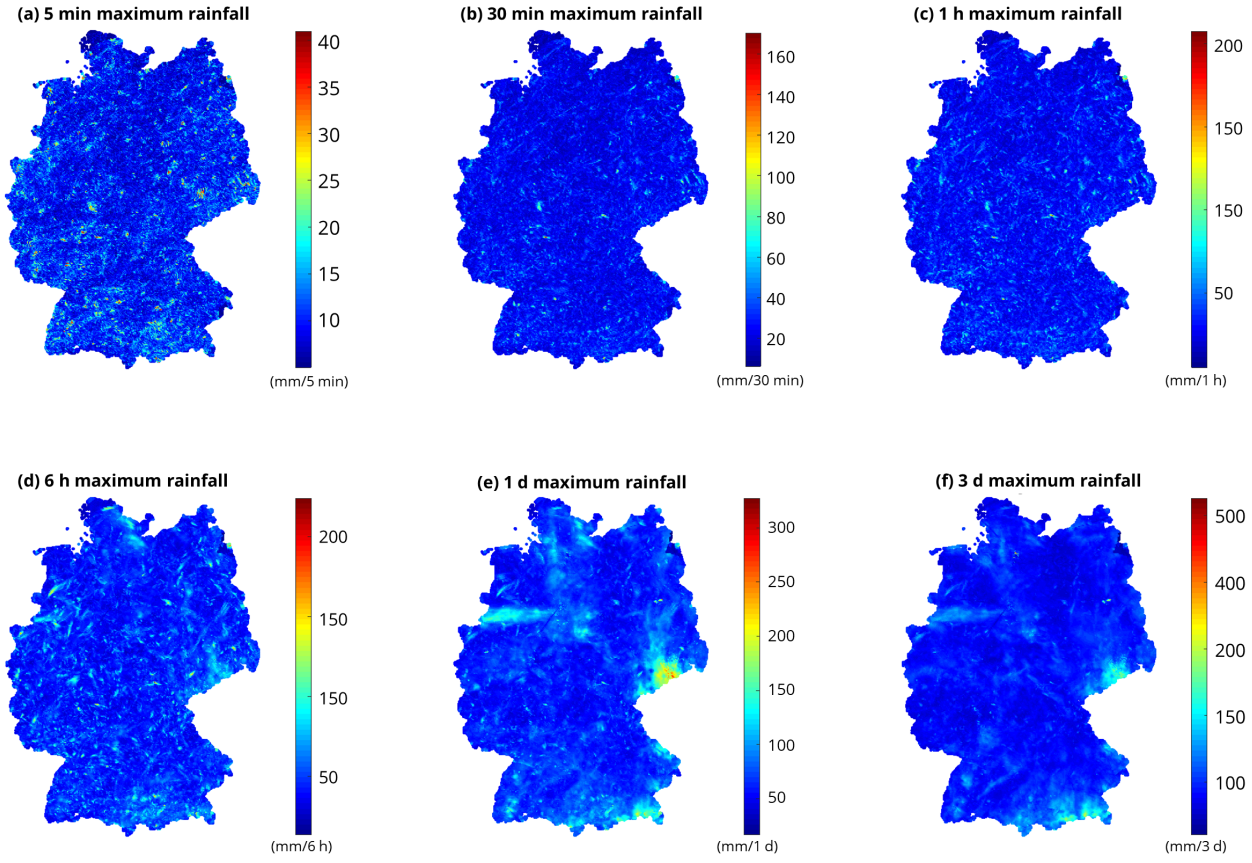

Figure 6. Spatial distribution of the maximum rainfall ~~with a given duration over Germany~~ values retrieved from QPE RADKLIM–YW (2001–2016) for different durations (5 min to 3 days).

3.3 Spatial distribution of maximum rainfall

Figure 6 shows the spatial distribution of 5 min, 30 min, 1 h, 6 h, 1 d, and 3 d maximum rainfall over Germany. The red and yellow spots that are spatially distributed in Fig. 6 (a) suggest that 5 min extreme rainfall can happen at any place in Germany. Note that extreme rain occurred also outside the Alpine region at the southern edge of Germany, which suggests that fine–scale extreme rainfall is not necessarily governed by topography. The influence of fine–scale intense rainfall persists until the hourly timescale as implied by the red and yellow hotspots that are similarly located in the maps of 5 min, 30 min, and 1 h. The distribution of maxima significantly changes for the 6 h duration (Fig. 6(d)), and an interesting pattern emerges in the map of 1 d and 3 d duration. These maxima seem to be dominated by single events ~~/single rainfall that has been really high~~or single heavy rainfall occurrence. Especially the 2002 flooding in Saxony (mid eastern edge) with ~~precedent~~ unprecedented longer heavy rainfall as well as one singular rainfall event in 2014 (narrow aisle in the Northwestern area) are clearly visible in the maps.

3.4 Scaling ~~behavior~~ behaviour at a single point

Figure 7 shows the maximum rainfall–duration relationship of the radar ~~rain cells~~ pixels at the major cities of Germany with a blue line as reference to see the differences better. Except for Hamburg and Stuttgart, most cities exhibit slight (Hannover, Kiel, Magdeburg, ~~Schwerin, Stuttugart~~Potsdam, Schwerin, Wiesbaden) to considerable (the remaining cities) deviation from a single power law ~~behavior~~behaviour. This significant deviation is similar to what was identified by ~~Galmarni et al. (2004) which~~ Galmarini et al. (2004) who found that the inflection of the curve is inevitable because of the small (or zero) rainfall observations attached to the maximum rainfall event. ~~This result also implies the real rainfall process significantly deviates from the assumptions of the simple rainfall models suggested by~~ Furthermore, Galmarini et al. (2004) and Zhang et al. (2013) ~~. Both studies~~ both showed that the maximum rainfall–duration relationship at a given point location ~~follow~~ follows a smooth and simple power law if the rainfall process can be ~~modeled~~ modelled with a set of simple stochastic processes. Our results imply that natural rainfall processes might significantly deviate from this rather simple assumption, also the model framework is also based on very few time series of very different lengths and resolutions.

3.5 Classification of maximum depth–duration relationship

The maximum ~~dept~~depth–duration relationships ~~in Fig. 7~~ for all pixels within Germany were clustered since ~~some show a similar shape with each other~~ Fig. 7 indicated that they might show similar shapes. The k–mean clustering algorithm ~~successfully~~ classified the depth–duration relationship into six categories revealing different curve characteristics regarding the curve shapes. Figure 8 shows a categorical map of Germany ~~indicating~~ representing each category with ~~a certain color and the~~ an individual colour. Additionally, depth–duration ~~relationship~~ relationships at 100 ~~grid cells randomly sampled~~ randomly chosen grid elements from each category are shown with the regression line from Category 5 as reference.

~~Cells~~ Pixels belonging to Category 1 have the highest rainfall intensities over all scales until 1 d and show a strong inflection at around 1 h similar to the scaling curve for whole Germany (Fig. 3). The ~~behavior~~ behaviour of the curve between 5 min and 1 h is associated with strong convective rainfall events ~~that pour for~~ of around 1~~h and move on or weaken~~ h within the corresponding pixel. Thus, these events are responsible for the high slope at the beginning part of the curve. Some curves also show another small inflection between 12 h and 1 d that might correspond to an inter storm arrival time over which another large event contributes to the positive slope of the curve at duration from 1 d and longer, or simply contributes to the general high intensity of the whole event. Category 1 ~~cells~~ pixels can be identified as yellow hotspots in Fig. 8 that occur predominantly as smaller ~~cells~~ pixels in the midst of Category 2 (red) and partly in Category 3 (~~lightpink) cell~~ light pink) pixel clusters. Category 2 ~~cells~~ pixels (red) have a similar curve shape as those in Category 1 and always occur together with Category 1 ~~cells~~pixels. The curve inflection begins around 30 min and the slope up to 3 d is a little ~~higher~~ steeper than Category 1's slope. This implies that unlike the hotspot locations, those locations experienced strong convective ~~pattern of a little~~ patterns of a slightly shorter duration, but potentially longer event durations in general. Most likely, Category 1 (event ~~center~~centre) and Category 2 (event boundary) ~~cells~~ pixels experience local convective events, which are forming in the summer months on warm days with a moist atmosphere. Categories 3 and 4 can be generally associated to large scale events dominated by regional weather patterns. The

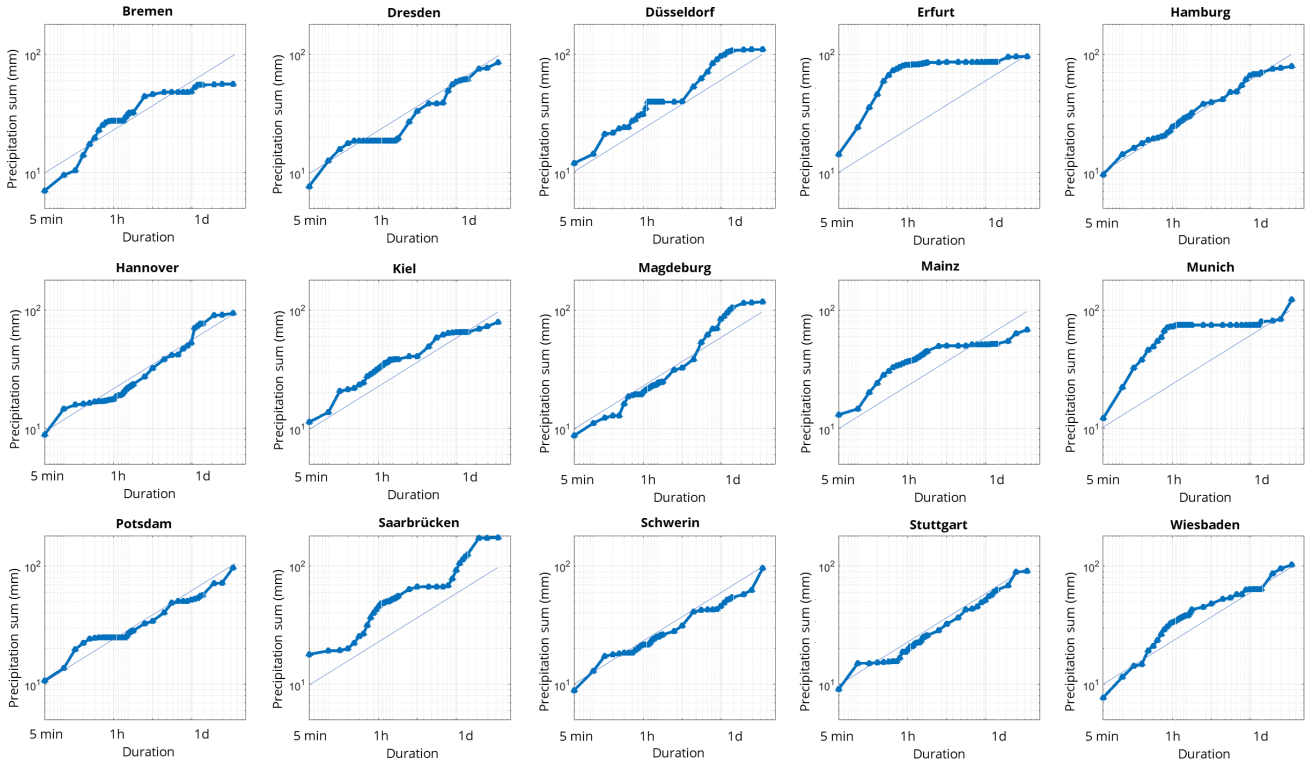

Figure 7. ~~Maximum depth~~Depth–duration ~~plot~~ relationships of ~~major cities~~ rain records for single pixels at rain gauge locations within state capitals of ~~Germany~~German federal states

three largest clusters in the map can be identified as intense frontal rainfall in August 2002 (Saxony, large cluster in Eastern Germany), heavy downpours over Münster in July 2014 (narrow path in the Northwestern part) and orographic rainfall in the Alpine region of southern Germany. In Category 3, curves show steep slopes up to one day that ~~are abruptly ending~~ abruptly end with super–daily duration. This category is contributing to the scales between 12 h and 3 d for the curve for whole Germany (Fig. 3). The steep slope at sub–daily duration is because the ~~cells~~ pixels experienced intense convective storms, however, with lower intensity than Categories 1 and 2. Yet, for daily–scale duration they can experience significant amounts of rainfall. Both Categories 4 and 5, which compose around 50 % of all ~~cells~~pixels, show rough power law ~~behavior~~ behaviour over all scales. Category 4 (dark blue) ~~cells~~ pixels are mainly at the outer borders of the described larger events as well as adjacent ~~cells~~ pixels of Categories 1 and 2. Thus, the curves have steep slopes because the corresponding ~~cells~~ pixels experienced great rainfall. Most ~~cells~~ pixels belong to Category 5 (36 %), showing the smoothest scaling ~~behavior~~ behaviour of all categories. ~~These~~ Based on the data set, these regions/locations never have been hit by any ‘extreme’ extreme event that could have altered the

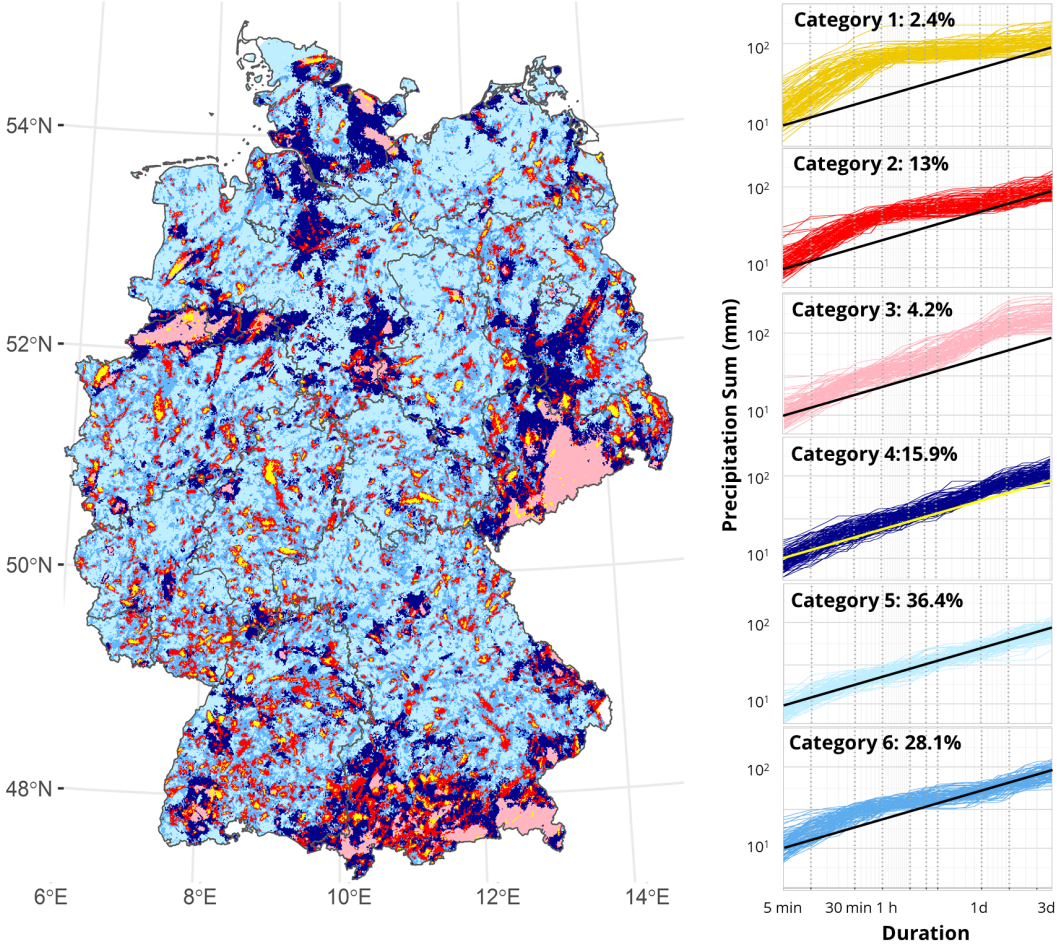

Figure 8. ~~Display of~~ Resulting 6 groups after clustering the ~~six categories of~~ maximum ~~rainfall~~ depth–duration relationships ~~a) spatially distributed over~~ of rainfall for all pixels. The left panel shows the ~~whole~~ spatial distribution of ~~Germany~~the groups, ~~and b) their~~ distinguishable by colour. The corresponding curve shapes ~~, sampled at~~ of 100 randomly selected radar ~~cells belonging to~~ pixels from each group are displayed on the ~~corresponding of~~ right side with the ~~six categories~~same colours as the map.

power law ~~behavior~~ behaviour of the depth–duration relationship. The locations of these ~~cells~~ pixels indicate no spatial pattern and can be seen as a kind of background ~~color~~ colour of the map. The last Category 6 contains similar characteristics from Categories 1 to 3 and comprises another 30 % of all ~~cells~~pixels. This category represents ~~cells~~ pixels experiencing common types of convective events with short heavy rainfall sequences on the sub–hourly scale, indicated by a relatively steep slope until 1 h compared to Categories 1 and 2. However, these ~~cells~~ pixels also experience longer rainfall sequences, thus showing an almost "three phase regime" as the overall curve for Germany with lower values. The found clusters can be further summarized into three classes: ~~Cells~~ Pixels that have experienced very heavy rainfall on a sub–hourly scale (Categories 1 and 2) exhibiting steep slopes at sub–hourly scale and mild slope for longer duration. The second class experienced heavy rainfall sequences of up to 1 d (Categories 3 and 4). The third type shows power law ~~behavior~~ behaviour over all scales and can be mainly found in Category 5. Category 6 simultaneously shows characteristics of Classes 1 and 2.

3.6 Sensitivity of scaling ~~behavior~~ behaviour to ground gauge network density

An important message from Sect. (3.4) and Sect. (3.5) is that the depth–duration relationship at a given point varies location by location based on the ~~rainstorms that the area experienced~~occurred rainstorms. This implies that the maximum depth–duration relationship over the entire study area, which is fundamentally the process of the superposition of these various relationships and the picking up of the very maximum values at each duration, may vary with regard to density and spatial formation of ground gauge networks (Sect. (3.5)). For this reason, we investigated how the depth–duration relationship would vary with regard to a different number of sampling pixels. Figure 9 shows the result corresponding to the pixel sample size of 10, 100, 1 000, and 10 000. For each of the cases, 30 ensembles of random pixel sampling were performed. For each of the plots, the maximum depth–duration relationship based on all radar pixels (n = 392 128) was shown for reference. Clear and smooth scaling ~~behaviors~~ behaviours are identified when the pixel sample size is 10 and 100, but the smooth scaling ~~behaviors~~ behaviours are lost when including more major rainfall events that formed the original maximum depth–duration relationship. This emphasizes that the number of rain gauges in a network is extremely relevant in order to adequately capture rainfall extremes. Note, most scaling relationships of the past including ~~Jennings (1950)~~ Jennings (1950) were based on the measurements of the ground gauge network. The station density was used as "best we could get" and was not tested against a smaller set of stations, as obviously including all reliable extremes improves the relationship. This might work for the Jennings curve as the global scale (~~sample size over a large space and maximum available time) makes~~ space and time) can make up for the limited spatial resolution. Regional scaling, however, suffers from the limited spatial extent, which cannot be completely balanced by a denser network or Radar data.

4 Conclusions

A thorough understanding on the scaling ~~behavior~~ behaviour of the depth–duration relationship of extreme precipitation has been limited because its high spatiotemporal variability cannot be fully captured by a measurement network composed of limited number of ground gauges. This study tried to overcome this limitation by using the radar Quantitative Precipitation

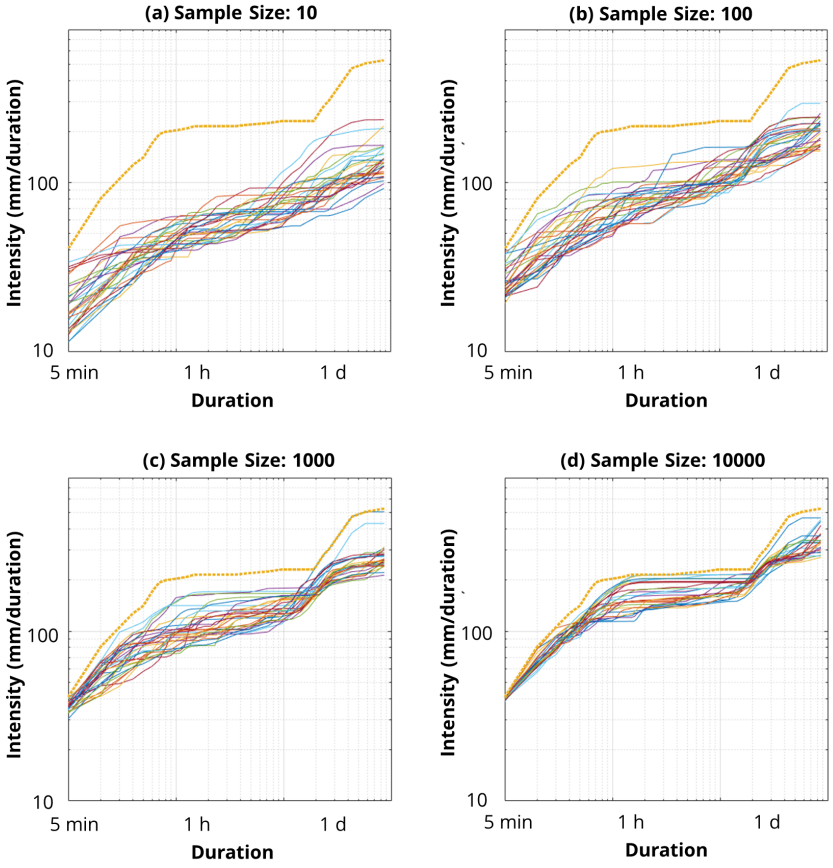

Figure 9. ~~Variation~~ Dependency of maximum depth–duration relationship ~~with varying~~ characteristic on underlying pixel sample size~~of~~. The maximum rainfall values are derived from (a) 10, (b) 100, (c) 1 000, and (d) 10 000 random pixels ~~used~~ from all considered pixels (n=392 128) within Germany. For each sample size, 30 ensembles are displayed and compared to ~~develop~~ the ~~relationship~~overall maximum curve from Fig. 3 and **??** (yellow top line in (a)–(d)).

Estimates (QPE) rainfall product RADKLIM–YW. The radar QPE enabled clear identification and explanation of the characteristics of the different scaling regimes of extreme rainfall depth–duration relationships. The maximum depth–duration relationship derived from radar data did not show clear scaling ~~behavior~~ behaviour compared to one based on gauge data from longer time series, but exhibited a "three phase regime" with a high slope at the duration smaller than 1 h, a plateau at the duration between 1 h and 1 d, and a low slope at the duration greater than 1 day. The relationship was developed based on only a few extreme rainfall events, which dominated the shape of the curve and this changed when examining quantiles of pixel maxima. The depth–duration relationship of lower quantile rainfall (e.g. 99 percentile) showed a smooth scaling ~~behavior~~ behaviour and the rainfall events contributing to the curve sparsely occurred at various locations of Germany. This implies that the modest extreme rainfall events are less sensitive to the random effects of a limited period (under sampling) and may even share common atmospheric conditions of rainfall generation regardless of pixel location in a limited region like Germany. The rainfall depth–duration relationship at a single radar pixel did not show clear power law ~~behavior~~ behaviour either. The shape of the curve was governed by the temporal structure of the extreme rainfall events ~~that the pixel experienced~~at the pixel location. The point wise clustering of depth–duration relationships revealed three classes of scaling ~~behavior~~behaviour: a) Linear scaling over all durations, as well as inflections at b) one hour and c) one day, which shows the influence of small convective ~~cells~~ pixels as well as large scale weather patterns on the depth–duration relationship. ~~Therefore, the scaling behavior at a given pixel location differed significantly location by location because each pixel experienced different extreme rainfall events~~The scaling behaviour thus can be significantly different for each pixel because the rainfall characteristics for each pixel are very different as well. Given that the extreme rainfall depth–duration relationship over a region is a process of overlapping the relationships observed at various pixel locations and picking up the highest rainfall values at each duration, the result implies that the depth–duration relationship of extreme rainfall can significantly deviate from power law ~~behavior~~behaviour. With longer available time series of radar in the future, the deviation can be further investigated and tested. Also, the known issue of rainfall extreme underestimation by RADKLIM–YW and the potential impact on the results need further evaluation.

Code and data availability. The data sets used in this study are freely available to download in ASCII and BINARY format and are published under the following DOI: 10.5676/DWD/RADKLIM_YW_V2017.002 (Winterrath et al., 2018b). Analysis was conducted in R (R Core Team, 2019) and Matlab with freely available R–packages ggplot (Wickham, 2016), RasterVis (Perpiñán and Hijmans, 2019), Rcpp–Roll (Ushey, 2018), and fst (Klik, 2019)

Author contributions. JP and DK conceptualized research, developed model code and methodology. JP carried out the analysis together with DK and RK. DK provided the computing facilities in his lab at Hongik University in South Korea. JP and DK prepared the manuscript with contribution from all co-authors. CB contributed the scientific idea, contributed to its refinement, to the discussion within the authors' group and to the writing.

Competing interests. There are no competing interests involved in this study.

Acknowledgements. The authors sincerely acknowledge the financial support by TU Dresden's Institutional Strategy, which is funded by the Excellence Initiative of the German Federal and State Governments. Professor Kim's contribution was supported by the Korea Environment Industry & Technology Institute (KEITI) through Water Management Research Program, funded by Korea Ministry of Environment (MOE) (Project No. 127557). We also thank Dr. Tanja Winterrath from the German Weather Service (DWD) for giving further insight on DWD's data processing. We thank four anonymous reviewers for their helpful comments and remarks to improve our manuscript.

References

Barbero, R., Fowler, H. J., Lenderink, G., and Blenkinsop, S.: Is the intensification of precipitation extremes with global warming better detected at hourly than daily resolutions?, Geophysical Research Letters, 44, 974–983, https://doi.org/10.1002/2016gl071917, 2017.

Blanchet, J., Ceresetti, D., Molinié, G., and Creutin, J.-D.: A regional GEV scale-invariant framework for Intensity–Duration–Frequency analysis, J. Hydrol., 540, 82–95, https://doi.org/10.1016/j.jhydrol.2016.06.007, 2016.

Borga, M., Gaume, E., Creutin, J. D., and Marchi, L.: Surveying flash floods: gauging the ungauged extremes, Hydrological Processes, 22, 3883–3885, https://doi.org/10.1002/hyp.7111, 2008.

Breña-Naranjo, J. A., Pedrozo-Acuña, A., and Rico-Ramirez, M. A.: World's greatest rainfall intensities observed by satellites, Atmos. Sci. Lett., 16, 420–424, https://doi.org/10.1002/asl2.546, 2015.

Commonwealth of Australia: Australia's Record Rainfall, online, http://www.bom.gov.au/water/designRainfalls/rainfallEvents/ausRecordRainfall.shtml, 2019.

Cristiano, E., ten Veldhuis, M.-C., and van de Giesen, N.: Spatial and temporal variability of rainfall and their effects on hydrological response in urban areas – a review, Hydrol. Earth Syst. Sci., 21, 3859–3878, https://doi.org/10.5194/hess-21-3859-2017, 2017.

Cristiano, E., ten Veldhuis, M.-C., Gaitan, S., Ochoa-Rodriguez, S., and van de Giesen, N.: Critical scales to explain urban hydrological response: an application in Cranbrook, London, Hydrol. Earth Syst. Sci., 22, https://doi.org/10.5194/hess-22-2425-2018, 2018.

Dao, D. A., Kim, D., Kim, S., and Park, J.: Determination of flood-inducing rainfall and runoff for highly urbanized area based on high-resolution radar-gauge composite rainfall data and flooded area GIS data, J. Hydrol., 584, 124 704, https://doi.org/10.1016/j.jhydrol.2020.124704, 2020.

DWA: Klimawandel erfordert wassersensible Stadtentwicklung, Korrespondenz Wasserwirtschaft, 8, 2015.

DWD: Nationaler Klimareport, 4. korrigierte Auflage, www.dwd.de/nationalerklimareport, 2020.

Dyck, S. and Peschke, G.: Grundlagen der Hydrologie, Verlag für Bauwesen, https://books.google.de/books?id=JYBZJgAACAAJ, 1995.

Fabry, F.: On the determination of scale ranges for precipitation fields, J. Geophys. Res. Atmos., 101, 12 819–12 826, https://doi.org/10.1029/96JD00718, http://doi.wiley.com/10.1029/96JD00718, 1996.

Fadhel, S., Rico-Ramirez, M. A., and Han, D.: Uncertainty of Intensity–Duration–Frequency (IDF) curves due to varied climate baseline periods, J. Hydrol., 547, 600–612, https://doi.org/10.1016/j.jhydrol.2017.02.013, https://ac.els-cdn.com/S0022169417300926/1-s2.0-S0022169417300926-main.pdf?_tid=cf511a0c-fad4-11e7-a06d-00000aacb361&acdnat=1516117938_9f0e0520549b5f62fb5ed0c6bde1bf1bhttp://www.sciencedirect.com/science/article/pii/S0022169417300926http://files/3593/Fa, 2017.

Gado, T. A., Hsu, K., and Sorooshian, S.: Rainfall frequency analysis for ungauged sites using satellite precipitation products, J. Hydrol., 554, 646–655, https://doi.org/10.1016/j.jhydrol.2017.09.043, https://doi.org/10.1016/j.jhydrol.2017.09.043, 2017.

Galmarini, S., Steyn, D. G., and Ainslie, B.: The scaling law relating world point-precipitation records to duration, Int. J. Climatol., 24, 533–546, https://doi.org/10.1002/joc.1022, 2004.

García-Marín, A. P., Ayuso-Muñoz, J. L., Jiménez-Hornero, F. J., and Estévez, J.: Selecting the best IDF model by using the multifractal approach, Hydrol. Process., 27, 433–443, https://doi.org/10.1002/hyp.9272, 2012.

Ghanmi, H., Bargaoui, Z., and Mallet, C.: Estimation of intensity-duration-frequency relationships according to the property of scale invariance and regionalization analysis in a Mediterranean coastal area, J. Hydrol., 541, 38–49, https://doi.org/10.1016/j.jhydrol.2016.07.002, 2016.

Gires, A., Tchiguirinskaia, I., Schertzer, D., Schellart, A., Berne, A., and Lovejoy, S.: Influence of small scale rainfall variability on standard comparison tools between radar and rain gauge data, Atmos. Res., 138, 125–138, https://doi.org/10.1016/j.atmosres.2013.11.008, 2014.

Gonzalez, S. and Bech, J.: Extreme point rainfall temporal scaling: a long term (1805–2014) regional and seasonal analysis in Spain, Int. J. Climatol., 37, 5068–5079, https://doi.org/10.1002/joc.5144, 2017.

Guerreiro, S. B., Fowler, H. J., Barbero, R., Westra, S., Lenderink, G., Blenkinsop, S., Lewis, E., and Li, X.-F.: Detection of continental-scale intensification of hourly rainfall extremes, Nature Climate Change, 8, 803–807, https://doi.org/10.1038/s41558-018-0245-3, 2018.

Hijmans, R., Garcia, N., and Wieczorek, J.: GADM: database of global administrative areas (http://gadm.org version 3.6), 2018.

Jennings, A. H.: WORLD ' S GREATEST OBSERVED POINT RAINFALLS, Mon. Weather Rev., 1950.

Kim, J., Lee, J., Kim, D., and Kang, B.: The role of rainfall spatial variability in estimating areal reduction factors, J. Hydrol., 568, 416–426, https://doi.org/10.1016/j.jhydrol.2018.11.014, 2019.

Klik, M.: fst: Lightning Fast Serialization of Data Frames for R, https://CRAN.R-project.org/package=fst, r package version 0.9.0 — For new features, see the 'Changelog' file (package source), 2019.

Kreklow, J., Tetzlaff, B., Kuhnt, G., and Burkhard, B.: A Rainfall Data Intercomparison Dataset of RADKLIM, RADOLAN, and Rain Gauge Data for Germany, Data, 4, 118, https://doi.org/10.3390/data4030118, 2019.

Lee, J., Ahn, J., Choi, E., and Kim, D.: Mesoscale Spatial Variability of Linear Trend of Precipitation Statistics in Korean Peninsula, Adv. Meteorol., 2016, 1–15, https://doi.org/10.1155/2016/3809719, 2016.

Lengfeld, K., Winterrath, T., Junghänel, T., Hafer, M., and Becker, A.: Characteristic spatial extent of hourly and daily precipitation events in Germany derived from 16 years of radar data, Meteorol. Z., pp. 363–378, https://doi.org/10.1127/metz/2019/0964, 2019.

Lengfeld, K., Kirstetter, P.-E., Fowler, H. J., Yu, J., Becker, A., Flamig, Z., and Gourley, J.: Use of radar data for characterizing extreme precipitation at fine scales and short durations, Environ. Res. Lett., 15, https://doi.org/10.1088/1748-9326/ab98b4, 2020.

Madsen, H., Arnbjerg-Nielsen, K., and Mikkelsen, P. S.: Update of regional intensity–duration–frequency curves in Denmark: Tendency towards increased storm intensities, Atmos. Res., 92, 343–349, https://doi.org/10.1016/j.atmosres.2009.01.013, 2009.

Marra, F. and Morin, E.: Use of radar QPE for the derivation of Intensity–Duration–Frequency curves in a range of climatic regimes, J. Hydrol., 531, 427–440, https://doi.org/10.1016/j.jhydrol.2015.08.064, 2015.

Marra, F., Morin, E., Peleg, N., Mei, Y., and Anagnostou, E. N.: Intensity-duration-frequency curves from remote sensing rainfall estimates: comparing satellite and weather radar over the eastern Mediterranean, Hydrol. Earth Syst. Sci., 21, 2389–2404, https://doi.org/10.5194/hess-21-2389-2017, 2017.

NWS: World record point precipitation measurements, http://www.nws.noaa.gov/oh/hdsc/record_precip/record_precip_world.html, 2017.

Overeem, A., Buishand, T. A., and Holleman, I.: Extreme rainfall analysis and estimation of depth-duration-frequency curves using weather radar, Water Resour. Res., 45, https://doi.org/10.1029/2009wr007869, 2009.

Papalexiou, S. M., Dialynas, Y. G., and Grimaldi, S.: Hershfield factor revisited: Correcting annual maximum precipitation, J. Hydrol., 542, 884–895, https://doi.org/10.1016/j.jhydrol.2016.09.058, 2016.

Paulhus, J. L. H.: INDIAN OCEAN AND TAIWAN RAINFALLS SET NEW RECORDS, Mon. Weather Rev., 93, 331–335, 1965.

Peleg, N., Ben-Asher, M., and Morin, E.: Radar subpixel-scale rainfall variability and uncertainty: lessons learned from observations of a dense rain-gauge network, Hydrol. Earth Syst. Sci., 17, 2195–2208, https://doi.org/10.5194/hess-17-2195-2013, 2013.

Peleg, N., Marra, F., Fatichi, S., Paschalis, A., Molnar, P., and Burlando, P.: Spatial variability of extreme rainfall at radar subpixel scale, J. Hydrol., 556, 922–933, https://doi.org/10.1016/j.jhydrol.2016.05.033, 2018.

Perpiñán, O. and Hijmans, R.: rasterVis, http://oscarperpinan.github.io/rastervis/, r package version 0.46 — For new features, see the 'Changelog' file (in the package source), 2019.

R Core Team: R: A Language and Environment for Statistical Computing, R Foundation for Statistical Computing, Vienna, Austria, https://www.R-project.org/, 2019.

Ralph E. Huschke, A.: Glossary of Meteorology, American Meteorology Society, Boston, 1959.

Rudolf, B. and Rapp, J.: Das Jahrhunderthochwasser der Elbe: Synoptische Wetterentwicklung und klimatologische Aspekte, Abdruck aus klimastatusbericht 2002, DWD, https://pdfs.semanticscholar.org/fdfc/a0eb2c7ac37d2d80ddd2700b3f710a7fed79.pdf, 2003.

Scott, A. J. and Knott, M.: A Cluster Analysis Method for Grouping Means in the Analysis of Variance, Biometrics, 30, 507–512, https://doi.org/10.2307/2529204, 1974.

Ushey, K.: RcppRoll: Efficient Rolling / Windowed Operations, https://CRAN.R-project.org/package=RcppRoll, r package version 0.3.0 — For new features, see the 'Changelog' file (in the package source), 2018.

Westra, S., Alexander, L. V., and Zwiers, F. W.: Global increasing trends in annual maximum daily precipitation, J. Clim., 26, 3904–3918, https://doi.org/10.1175/JCLI-D-12-00502.1, 2013.

Westra, S., Fowler, H. J., Evans, J. P., Alexander, L. V., Berg, P., Johnson, F., Kendon, E. J., Lenderink, G., and Roberts, N. M.: Future changes to the intensity and frequency of short-duration extreme rainfall, Rev. Geophys., 52, 522–555, https://doi.org/10.1002/2014rg000464, 2014.

Wickham, H.: ggplot2: Elegant Graphics for Data Analysis, Springer-Verlag New York, https://ggplot2.tidyverse.org, 2016.

Winterrath, T., Brendel, C., Hafer, M., Junghänel, T., Klameth, A., Walawender, E., Weigl, E., and Becker, A.: Erstellung einer radargestützten Niederschlagsklimatologie, 2017.

Winterrath, T., Brendel, C., Hafer, M., Junghänel, T., Klameth, A., Lengfeld, K., Walawender, E., Weigl, E., and Becker, A.: Radar climatology (RADKLIM) version 2017.002: Reprocessed gauge-adjusted radar data, one-hour precipitation sums (RW), https://doi.org/10.5676/dwd/radklim_rw_v2017.002, 2018a.

Winterrath, T., Brendel, C., Hafer, M., Junghänel, T., Klameth, A., Lengfeld, K., Walawender, E., Weigl, E., and Becker, A.: Radar climatology (RADKLIM) version 2017.002: Reprocessed quasi gauge-adjusted radar data, 5-minute precipitation sums (YW), https://doi.org/10.5676/dwd/radklim_yw_v2017.002, 2018b.

World Meteorological Organization: Guide to hydrological practices, 1994.

Yang, Z.-Y., Pourghasemi, H. R., and Lee, Y.-H.: Fractal analysis of rainfall-induced landslide and debris flow spread distribution in the Chenyulan Creek Basin, Taiwan, J. Earth Sci., 27, 151–159, https://doi.org/10.1007/s12583-016-0633-4, 2016.

Zhang, H., Fraedrich, K., Zhu, X., Blender, R., and Zhang, L.: World's Greatest Observed Point Rainfalls: Jennings (1950) Scaling Law, J. Hydrometeorol., 14, 1952–1957, https://doi.org/10.1175/JHM-D-13-074.1, 2013.